Published in final edited form as:
Circ Res. 2012 July 20; 111(3): 322–332. doi:10.1161/CIRCRESAHA.112.265173.

Blocking *SCN10A* channels in heart reduces late sodium current and is antiarrhythmic

Tao Yang[1,2], **Thomas C. Atack**[1], **Dina Myers Stroud**[1], **Wei Zhang**[1], **Lynn Hall**[1], and **Dan M. Roden**[1,2]

[1]Department of Medicine, Vanderbilt University School of Medicine, Nashville, Tennessee, USA

[2]Department of Pharmacology, Vanderbilt University School of Medicine, Nashville, Tennessee, USA

Abstract

Rationale—While the sodium channel locus *SCN10A* has been implicated by genome-wide association studies as a modulator of cardiac electrophysiology, the role of its gene product Nav1.8 as a modulator of cardiac ion currents is unknown.

Objective—We determined the electrophysiological and pharmacological properties of Nav1.8 in heterologous cell systems and assessed the antiarrhythmic effect of Nav1.8 block on isolated mouse and rabbit ventricular cardiomyocytes.

Methods and results—We first demonstrated that *Scn10a* transcripts are identified in mouse heart and that the blocker A-803467 is highly specific for Nav1.8 current over that of Nav1.5, the canonical cardiac sodium channel encoded by *SCN5A*. We then showed that low concentrations of A-803467 selectively block “late” sodium current and shorten action potentials in mouse and rabbit cardiomyocytes. Exaggerated late sodium current is known to mediate arrhythmogenic early afterdepolarizations in heart, and these were similarly suppressed by low concentrations of A-803467.

Conclusion—*SCN10A* expression contributes to late sodium current in heart, and represents a new target for antiarrhythmic intervention.

Keywords

SCN10A; sodium channels; heart; afterdepolarizations; arrhythmia

Introduction

The opening of sodium channels initiates action potentials in most cardiac cells. The canonical cardiac sodium channel, Nav1.5, is encoded by *SCN5A*, and Nav1.5 blockers reduce sodium current (I_{Na}) in individual cells and conduction velocity in the heart.[1] The latter action can be antiarrhythmic, but can also provoke arrhythmias, likely by engaging reentrant circuits. Mutations in *SCN5A* cause a range of human disease including type 3 long QT syndrome characterized by defective fast inactivation, enhanced “late” sodium current ($I_{Na\text{-}L}$) during the plateau of the action potential, prolonged action potential duration (APD), and arrhythmogenic early afterdepolarizations (EADs).[2]

Address correspondence to: Dr. Dan M. Roden, 1285 MRB-4, 2215B Garland Avenue, Vanderbilt University School of Medicine, Nashville, Tennessee 37232, Tel: 615-322-0067, dan.roden@vanderbilt.edu.

DISCLOSURES
None

The idea that sodium channels may not inactivate completely after opening was recognized in the node of Ranvier in the mid-1970s,[3] and a late plateau current in heart sensitive to the sodium channel specific toxin tetrodotoxin (TTX) was identified shortly thereafter.[4–6] This late sodium current represents either channels that do not inactivate completely after opening or a "window" current flowing in the restricted voltage range where channels are activated and also not completely inactivated. The plateau current is sensitive not only to TTX but also to clinically used antiarrhythmics and other agents,[7–9] including the antianginal ranolazine;[10] this effect of ranolazine is not specific for *SCN5A* channels, as the drug is known to block multiple other voltage-gated sodium channel isoforms.[11–13]

The genome-wide association study (GWAS) paradigm has been used to examine variability in PR and QRS durations, electrocardiographic indices of atrioventricular and intraventricular conduction velocity, respectively.[14–18] In both cases, the top associations have been with common single nucleotide polymorphisms (SNPs) not in *SCN5A*, but in a directly adjacent gene, *SCN10A*, which encodes the Nav1.8 channel known to be expressed in dorsal root ganglia (DRG)[19, 20] and in retina,[21] but not previously implicated in cardiovascular function.

Preliminary studies[14] included in one of the PR GWAS reports detected expression of the gene by PCR in mouse and human heart, and indicated shorter PR interval, but no effect on QRS duration, in *Scn10a*$^{-/-}$ mice. By contrast, the QRS meta-analysis reported[18] that the Nav1.8 blocker A-803467[22] prolonged both PR and QRS in wild-type mice, and that the gene was expressed in heart and highly enriched in cells isolated from the conduction system. Notably, cells in the conduction system have the longest action potentials in the heart and a physiologic $I_{Na\text{-}L}$ may contribute.23, 24 Our findings here demonstrate that Nav1.8 channels contribute to $I_{Na\text{-}L}$ in heart and that Nav1.8 block suppresses arrhythmogenic afterdepolarizations. These results not only reveal a direct role for *SCN10A* expression in cardiac electrophysiology but also identify its gene product as a potential target for antiarrhythmic intervention.

Methods

FuGENE6-mediated channel expression and cell transfection

ND7/23 cells (Sigma-Aldrich, St. Louis, MO), a cell line formed by fusion between mouse neuroblastoma and rat DRG cells,[25] were cultured in Dulbecco's modified Eagle's medium (DMEM, Invitrogen, Carlsbad, CA) supplemented with 10% fetal bovine serum (Invitrogen), 2 mM L-glutamine, 100 U/ml penicillin and 100 μg/ml streptomycin at 37°C under 95% air+5% CO_2. After growth to ~70% confluence on 35-mm polystyrene culture dishes in culture, cells were transiently transfected as follows: 2–3 μg of the cDNA encoding human *SCN10A* or *SCN5A* (plus 0.5 μg of a plasmid for green fluorescent protein, GFP) were mixed with 10 μl FuGENE6 (Roche) in 0.5 ml serum free DMEM medium and incubated for 30 minutes, after which the standard medium was replaced for a 48 hour incubation. GFP was used as a marker to identify successfully transfected cells for the electrophysiology studies. The cells were harvested by brief wash-off without trypsinization, and stored in standard medium for use within 12 hours.

Isolation of mouse and rabbit ventricular cardiomyocytes

Adult mouse and rabbit cardiac ventricular myocytes were isolated by a modified collagenase/ protease method (Supplemental Methods);[26] in these studies, we used mice in which the murine gene has been ablated and the human cardiac sodium (H) channel gene has been placed in the murine Scn5a locus.[27] We have previously shown that these H/H mice display sodium current and electrocardiograms identical to those from wild-type mice.[27] All

procedures were approved by the Institutional Animal Care and Use Committee. For electrophysiology experiments, mice (twelve wild-type and three *scn10a*$^{-/-}$) and rabbits (5) were used.

Ion current recordings

The biophysical properties of sodium currents were determined by voltage clamp protocols shown in the figures. Voltage dependence of inactivation was studied using 500-ms prepulses from −120 to −20 mV in 10-mV increments, followed by a 100-ms test pulse to +20 mV (for the Nav1.8 channel) or −20 mV (for the Nav1.5 channel). Two types of voltage-clamp experiments were conducted. First, we applied regular 200-ms square-wave pulses to record peak and late I_{Na} in mouse or rabbit ventricular myocytes prior toand during drug application. The second protocol was a slow ramp to specifically examine late current without the need for a previously depolarizing pulse; this approach allows the experiment to be conducted in physiologic extracellular sodium concentration. In both instances, the perfusate contained 1 μM nisoldipine and 200 μM $NiCl_2$ to block other inward current through L- and T-type calcium channels.

Current-voltage relations for steady-state activation and inactivation were determined by fitting a Boltzmann function ($I/Imax = [1 + \exp((V - V_{1/2}) / k)]^{-1}$), yielding the membrane potential of the half-maximal activation ($V_{1/2}$-activation) and inactivation ($V_{1/2}$-inactivation) and slope factor (k). The time course of inactivation of macroscopic current was fit with a monoexponential Chebyshev equation: $I=A_1{}^{*}\exp[-(t-k)/r_1]+C$.

Action potential recordings

To record action potentials from isolated ventricular myocytes, cells were studied in current-clamp mode (Axopatch 200B amplifier, Molecular Diagnostics, Sunnyvale, CA) by injecting stimulus current (1–2 nA, 2–4 ms) at different frequencies (5, 2, 1 and 0.1 Hz). Junction potentials between pipette and bath solutions were compensated electronically.

Data acquisition was carried out using an Axopatch 200B patch-clamp amplifier and software pCLAMP 9.2. Currents were filtered at 5 kHz (−3 dB, four-pole Bessel filter) and digitized using an analog-to-digital interface (Digidata 1322A, Molecular Diagnostics). To minimize capacitive transients, capacitance was compensated ~80%. Series resistance was 1–4 MΩ. In all voltage-clamp experiments, the protocols are presented schematically in the figures. Linear leakage currents were digitally subtracted online by the P/N protocol. All ion currents and action potential (AP) parameters were analyzed using pCLAMP9.2 software.

RNA isolation and Real-time Polymerase Chain Reaction (PCR)

The detailed methods are presented as online supplemental data.

Solutions and drugs

To record Nav1.8 and Nav1.5 currents transiently expressed in ND7/23 cells, we used an external K^+-free solution that contained (in mmol/L): 135 NaCl, 1.8 $CaCl_2$, $MgCl_2$ 1.0, TEA-Cl, 10 HEPES and 10 glucose, with a pH of 7.4 adjusted with NaOH. Endogenous TTX-sensitive I_{Na} and L-/T-type I_{Ca} were eliminated with tetrodotoxin 200 nM, nisoldipine 0.5 μM and $NiCl_2$ 200 μM, respectively. Glass electrodes were filled with the internal solution which contained (in mmol/L): 120 CsF, 10 NaCl, 1 $CaCl_2$, 1 $MgCl_2$, 10 EGTA, 10 TEA-Cl and 10 HEPES, with a pH of 7.3 adjusted with CsOH. To better control I_{Na} recording in mouse and rabbit ventricular myocytes, the internal and external Na^+ concentrations were lowered to 5 and 20 mmol/L, respectively. The experiments for I_{Na} recordings in mycoytes were conducted at 18 °C. Other experiments were done at 22~23 °C.

To record the action potentials in mouse and rabbit ventricular myocytes, external Tyrode's solution contained (in mmol/L): 135 NaCl, 4 KCl, 1.8 $CaCl_2$, and 1 $MgCl_2$, 5 HEPES and glucose 10, with a pH of 7.4 (adjusted by NaOH). The pipette (intracellular) solution had (in mmol/L): 120 Aspirate-K, 25 KCl, 4 ATP-Na_2, 1 $MgCl_2$, 2 Phosphocreatine-Na_2, 2 GTP-Na, 1 $CaCl_2$, 10 EGTA and 5 HEPES, with a pH of 7.3 (adjusted by KOH). A-803467, a specific SCN10A channel blocker, was purchased from Sigma-Aldrich Corp. (St. Louis. MO) and dissolved in 5% dimethyl sulfoxide (DMSO) and 95% polyethylene glycol (PEG 400)[28] to make a stock solution of 1 mmol/L. During the experiments, the drug solution was further diluted at the desired test concentrations. The final concentrations of solvents in the cell chamber were 0.01% or less, with no effects on Nav1.8 and action potentials in separate experiments. For experiments in which the antiarrhythmic effect of Nav1.8 block was examined, the external Tyrode's solution with lower external potassium (2 mmol/L) and a low concentration of ATX-II (3–5 nmol/L) was used to induce EADs.

Experiments evaluating the effects of drug were conducted by first establishing a pre-drug stable baseline and then adding drug to the extracellular solution until a new steady state was evident during repetitive pulsing. In the experiments shown in Figure 7I, rabbit ventricular myocytes were pretreated with A-803467 prior to ATX-II.

Generation of Scn10a$^{-/-}$ mice

Founder mice were regenerated by MRC Harwell using the same construct as previously reported.[29] Mice were genotyped using PCR amplification of fragment that includes the targeted region: a 1100 bp band was seen in wild type mice and a 900 bp band in the Scn10a$^{-/-}$ mice. Ventricular myocytes were isolated and studied using the same procedures as those outlined above.

Statistical analysis

Results are presented as mean ± SEM, and statistical comparisons were made using the unpaired and paired Student's *t*-test. A value of $P<0.05$ was considered statistically significance. Statistical significance for quantitative real-time PCR was determined by the Wilcoxon Rank Sum test.

RESULTS

Contrasting electrophysiologic and pharmacologic properties of Nav1.8 and Nav1.5 in a heterologous expression system

As previously reported,[30] expression of *SCN10A* in CHO or HEK cells, heterologous systems conventionally used to study *SCN5A*, yielded very small and inconsistent currents, even with coexpression of any of the four sodium channel β-subunits or incubation at low temperatures. However, in ND7/23 cells (a cell line formed by fusion between mouse neuroblastoma and rat DRG cells), robust currents were readily detected[28]. We confirmed expression of the construct and the absence of any endogenous *SCN10A* by RT-PCR (Supplemental Figure I). These cells do express a TTX-sensitive channel so all the experiments reported here were conducted in the presence of a low concentration (200 nM) of TTX. Both Nav1.5 and Nav1.8 are designated TTX-resistant because a high concentration (30 μM) is required to suppress Nav1.5 current and does not affect Nav1.8 currents. In addition, the cells express both β1 and β3 sodium channel subunits.[25]

Figure 1 shows currents recorded with transfection of *SCN10A* or *SCN5A* in ND7/23 cells. The *SCN5A*-mediated current displays fast activation and inactivation typical for Nav1.5 current (and shown in Figure 1A) recorded in other cells transfected with *SCN5A* plus *SCN1B*, encoding the β1 subunit. By contrast, *SCN10A*-mediated current activates and

inactivates much more slowly. Online Table I (contrasts the Nav1.5 and Nav1.8 currents in ND7/23 cells. Not only is the time to peak Nav1.8 current strikingly delayed compared to that for Nav1.5, but the post-peak (late) current also represents a much larger fraction of peak current than with Nav1.5. In addition, Nav1.8 channels activate at much more positive potentials than do Nav1.5 channels; the peak current amplitudes were at ~+20mV compared to ~−30mV for Nav1.5. Both channels displayed an overlap of activation and inactivation voltage relationships that would enable a "window" current, but in different voltage ranges (Figure 1E).

Figures 2A and 2B show the selectivity of the blocker A-803467 for Nav1.8 over Nav1.5 currents in this system. Single 50-ms repetitive pulses from −120 mV to +20 mV (the potential at which peak Nav1.8 current is observed) were used to elicit Nav1.8 current, and block was near-complete with 30 nM A-803467 (Figure 2A). However, this concentration of drug produced no effect on Nav1.5 current studied with single pulses to −30 mV (the potential at which peak Nav1.5 current is recorded). Indeed, even at 1000 nM, the blocker had minimal effect on Nav1.5 current (Figure 2B). No effect of A803467 on peak sodium current was also seen in mouse cardiomycytes (Supplemental Figure IIA).

As described below, experiments using A-803467 in cardiomyocytes implicated *SCN10A* as a mediator of late I_{Na}. However, late I_{Na} is commonly more sensitive to drug block than is peak I_{Na}. Accordingly, we conducted further experiments to examine the effects of A-803467 on physiologic and pathologically-increased Nav1.5-mediated late current. Figure 2C shows that in ND7/23 cells, application of the sodium channel opener ATX-II augments Nav1.5-mediated sodium current but that this augmented current is not highly sensitive to A-803467: ATX-augmented *SCN5A*-mediated late current was no more sensitive to A-803467 than was peak current (50% block at ~5000 nM). Another setting in which SCN5A-mediated late current is pathologically enhanced is in type 3 long QT syndrome. Figure 2D shows that 1000 nM A-803467 had no effect on late currents recorded with heterologous expression of LQT3 mutant *SCN5A* channel F1486L; the same lack of effect on LQT3 late current was observed with the mutants R1544H and T1304. This blocker at high concentrations (1 and 10 μmol/L) also had minor effect on L-type calcium current in mouse myocytes (Supplemental Figure IIB).

We also examined the relative abundance of Scn10a transcripts in mouse heart compared to those for human cardiac sodium channel allele by quantitative RT-PCR (Figure 3). *Scn10a* transcripts are readily detected in both atria and right ventricle but were markedly reduced in left ventricle. The ND7/23 cell data and the expression data establish low-dose A-803467 as a tool to dissect the contribution of *SCN10A* to ionic currents recorded in cardiomyocytes.

A component of sodium current in cardiomyocytes is sensitive to low concentrations of A-803467

Figure 4A shows the effects of A-803467 (30 nM) on peak and late sodium current in mouse ventricular myocytes. The right hand panels contrast, at expanded scales, the prominent suppression of late current with minimal effects on peak current; late currents such as these were observed in approximately half of the cells studied. A 2-sec voltage command ramp from −120 mV to +40 mV (Figure 4B) elicited an inward current with two minima, one at ~ −70 mV and the second at ~−10 mV. A-803467 reduced the component at the more positive potential, and the A-803467 sensitive-current obtained by digital subtraction is shown as difference current. Data summarizing the effect of A-803467 on these two minima in the ramp current are presented in Figure 4C and 4D; the drug reduced current at −70 mV by 7.3±1.3% and at 0 mV by 39.2±6.2% (n=8, $p<0.01$). These data further confirm that Nav1.8 current contributes to late sodium current (I_{Na-L}) in heart.

A-803467 shortens ventricular APD and suppresses EADs

Figure 5 shows the effects of 30 nM A-803467 on action potentials recorded in mouse ventricular myocytes. The drug produced little effect at fast rates (5 and 1 Hz), but at slower ones, action potential shortening was evident (right, Figure 5A). The effects on APD at 50% and 90% repolarization (APD_{50} and APD_{90}) in individual cells (n=20) are shown in Figures 5B–E: these differences are statistically significant at slower rate, although no effect by A-803467 was observed in 9/20 cells. This is consistent with the notion that $I_{Na\text{-}L}$ is a more prominent contributor to action potential duration at slow rather than at fast rates, and that not all ventricular myocytes express *Scn10a*.

Figure 6 shows the results of experiments conducted in rabbit myocytes. As in mouse cells, 30 nM A-803467 preferably inhibited late current during 200-ms pulsing and had only a minor effect on peak current in rabbit cardiomyocytes. The drug-sensitive component (as difference current) was separated from the mixed sodium currents by digital subtraction (Figure 6A and insets). The difference current displays very slow activation and inactivation with prominent late current, features similar to those seen with heterologous expression of SCN10A in ND7/23 cells.

Figure 6B shows action potential traces in a rabbit ventricular myocyte recorded at 2 Hz prior to and during exposure to 30 nM A-803467, which shortened APD. The effect on APD_{50} and APD_{90} in seven rabbit myocytes are summarized in Figure 6C.

The action potential prolongation generated by enhanced $I_{Na\text{-}L}$ can generate EADs that have been implicated in arrhythmias in both congenital long QT syndromes[31] and in acquired settings.[32, 33] We exposed myocytes to a low concentration of ATX-II and then demonstrated that 30 nM A-803467 suppressed EADs elicited under these conditions in mouse and rabbit myocytes. Figure 7A shows action potentials in a mouse myocyte recorded under EAD-promoting conditions: low extracellular potassium (2 mM) and exposure to a low concentration (3 nM) of the sodium channel opener ATX-II. Using 1 Hz stimulation rate under these conditions elicited EADs and triggered activity (Figure 7B–D) and these abnormal action potentials were promptly suppressed by 30 nM A-803467. This effect was observed in 7/8 mouse preparations.

Very similar effects were observed in rabbit myocytes (Figure 7G–I). Exposure to 5 nM ATX-II for 15 minutes induced EADs that lasted longer than the drive cycle length (Figure 7H). When the cell was pretreated with A-803467 for 15 minutes, addition of 5 nM ATX-II did not cause long-lasting EADs, although the recorded action potentials still were much longer than that in control (indicated by an arrow in Figure 7I).

Effects of A-803467 in Scn10a$^{-/-}$ mouse cardiomyocytes

Figure 8 shows that in ventricular myocytes isolated from *Scn10a*$^{-/-}$ mice, no late sodium current was recorded and there was no effect of 30 nM A-803467 on current recorded at the peak or at 200 msec after the onset of the depolarizing pulse. Action potentials were shorter than those in wild-type animals, and there was similarly no effect of A-803467 on APD.

DISCUSSION

One of the key scientific advances enabled by the GWAS paradigm is the identification of genes and pathways contributing to important human phenotypes and not previously implicated in human physiology.[34] GWAS provides a very robust and reproducible signal that variation at the *SCN10A* locus, not previously implicated in cardiac physiology, modulates conduction in the heart. However, a function of the *SCN10A* gene product Nav1.8 in cardiac electrophysiology had not, to date, been defined. We used the Nav1.8-

specific blocker A-803467 to not only define a role of Nav1.8 channels in control of the cardiac action potential but also to demonstrate that block of Nav1.8-mediated current can exert antiarrhythmic actions.

One hurdle that we had to overcome in these experiments was to identify and validate a system to compare Nav1.5 and Nav1.8 pharmacology. Cell lines that routinely generate robust Nav1.5 currents with transfection did not generate similar Nav1.8 currents. The likely explanation for this finding is that ND7/23 cells express some key but as yet unidentified cofactor necessary for Nav1.8 expression and absent from HEK or CHO cells. The major findings in the ND7/23 experiments we present are that A-803467 is specific for Nav1.8 over Nav1.5, and that the channels display striking differences in gating and late current.

While our findings demonstrate a role for Nav1.8 in the control of cardiac repolarization as assessed by action potential duration, the GWAS results implicate variants in *SCN10A* as modulators of cardiac conduction. The functional characteristics of Nav1.8 current in the heterologous expression experiments indicate that the current activates much more slowly than does Nav1.5 current, and this difference may in turn contribute to variable cell-to-cell charge transfer that underlies fast conduction in heart. Available data raise the possibility that the *SCN10A* signal may be mediated by a non-synonymous coding region SNP, resulting in V1073A. Preliminary reports indicate V1073A does demonstrate gating characteristics that differ from the wild-type channel[35] but these experiments have only been conducted in heterologous expression systems and so the way in which this variant modulates Nav1.8 function awaits further studies in myocytes.

The quantitative RT-PCR data unexpectedly show that *Scn10a* expression is much higher in right compared to left ventricle. It is conceivable that this signal reflects enrichment in specialized cell types (e.g. conduction tissue). Indeed, the QRS GWAS report included data that expression was enriched in mouse cardiac Purkinje cells compared to ventricle;[18] Purkinje cells have longer action potentials than those in ventricle so it is conceivable that Nav1.8 contributes to this difference. We only observed a late current sensitive to 30 nM A-803467 in about half of the myocytes we studied consistent with the idea that many myocytes will lack Nav1.8 expression. In the electrophysiologic experiments, we did not distinguish myocytes of left versus right ventricular origin.

Interestingly, while Nav1.5 is the canonical cardiac sodium channel, other channels are known to be expressed at lower levels and in specific regions in heart.[36, 37] One report indicates that Nav1.8 is detectible in heart and peri-cardiac ganglia by immunostaining,[38] but using Western analyses we have been unable to establish the specificity of any commercially available antibody. Thus, a key unanswered question is the cellular and subcellular localization of the Nav1.8 channel in heart and other tissues. The possibility remains, for example, that the GWAS conduction velocity signal reflects neural modulation of cardiac conduction by Nav1.8 channels expressed in cardiac ganglia. Further, our data (Figure 5, B–E) indicate that the extent to which A-803467 shortens action potential duration varies from cell to cell, suggesting that the current plays a variable role, perhaps across cell subtypes, in cardiac repolarization. The qRT-PCR data demonstrate that there is striking variability in the detection of *Scn10a* transcripts across chambers, but do not address cell-type specific expression of the gene.

A low concentration of A-803467 suppressed EADs and associated triggered activity. ATX-II interferes with inactivation of multiple sodium channel isoforms, including Scn5a. However, the antiarrhythmic effect of A-803467 cannot be attributed to block of Nav1.5 channels because we have shown that the concentration used is far below that required to even minimally block physiologic or pathologic late Nav1.5 current. Thus, we infer that the

effect of A-803467 in this setting is to eliminate a component of arrhythmogenic inward current – presumably mediated by Nav1.8 – to a sufficient extent to suppress EADs and triggering. The failure of A-803467 to alter APD in multiple ventricular myocytes from $Scn10a^{-/-}$ mice lends further support to this hypothesis.

The demonstration that Nav1.8 channels play a role in cardiac repolarization and that Nav1.8 block can suppress arrhythmogenic EADs represents a key proof-of-principle finding for further development of this novel antiarrhythmic strategy. Many currently available antiarrhythmics block both peak and late current mediated by Nav1.5,[7, 8] but these can provoke arrhythmias.[39] Ranolazine appears to be more selective for late current,[10] and to date, less proarrhythmic.[40, 41] Indeed, ranolazine exerts antiarrhythmic effects in some settings,[42–44] including suppressing EADs. However, the drug is not selective for Nav1.5 currents. The interesting difference between Nav1.5 and Nav1.8 activation raises the possibility that selective block of late Nav1.8-mediated current could be antiarrhythmic without proarrhythmic liability.

Supplementary Material

Refer to Web version on PubMed Central for supplementary material.

Acknowledgments

DRG tissue was supplied by Dr. Bruce Carter at Vanderbilt University. We also acknowledge the assistance of our Vanderbilt colleagues Alfred George, Bjorn Knollmann, Melissa Ryan, and Eleonora Savio Galimberti in providing isolated mouse and rabbit myocytes.

SOURCES OF FUNDING

This work was supported by a grant from the U.S. National Institutes of Health (HL49989).

Non-standard Abbreviations

ND7/23	a dorsal root gnglion derived cell line
APD	action potential duration
EAD	early afterdepolarization
TTX	tetrodotoxin
GWAS	genome-wide association study
SNPs	single nucleotide polymorphisms
DRG	dorsal root ganglia
$I_{Na\text{-}L}$	“late” sodium current
H/H	humanized sodium channel
WT	wild type

References

1. Remme CA, Bezzina CR. Sodium channel (dys)function and cardiac arrhythmias. Cardiovasc Ther. 2010; 28:287–294. [PubMed: 20645984]
2. Wilde AA, Brugada R. Phenotypical manifestations of mutations in the genes encoding subunits of the cardiac sodium channel. Circulation Research. 2011; 108:884–897. [PubMed: 21454796]
3. Dubois JM, Bergman C. Late sodium current in the node of ranvier. Pflugers Arch. 1975; 357:145–148. [PubMed: 1080274]

4. Carmeliet E. Slow inactivation of the sodium current in rabbit cardiac purkinje fibres. Pflugers Arch. 1987; 408:18–26. [PubMed: 2434919]

5. Coraboeuf E, Deroubaix E, Coulombe A. Effect of tetrodotoxin on action potentials of the conducting system in the dog heart. American Journal of Physiology. 1979; 236:HV561–HV561.

6. Gintant GA, Datyner NB, Cohen IS. Slow inactivation of a tetrodotoxin-sensitive current in canine cardiac purkinje fibers. Biophysical Journal. 1984; 45:509–512. [PubMed: 6324914]

7. Nagatomo T, January CT, Makielski JC. Preferential block of late sodium current in the lqt3 deltakpq mutant by the class i(c) antiarrhythmic flecainide. Mol Pharmacol. 2000; 57:101–107. [PubMed: 10617684]

8. Sunami A, Fan Z, Sawanobori T, Hiraoka M. Use-dependent block of na+ currents by mexiletine at the single channel level in guinea-pig ventricular myocytes. Br J Pharmacol. 1993; 110:183–192. [PubMed: 8220878]

9. Delpon E, Tamargo J, Sanchez-Chapula J. Further characterization of the effects of imipramine on plateau membrane currents in guinea-pig ventricular myocytes. Naunyn Schmiedebergs Arch Pharmacol. 1991; 344:645–652. [PubMed: 1775197]

10. Zaza A, Belardinelli L, Shryock JC. Pathophysiology and pharmacology of the cardiac “late sodium current”. Pharmacol Ther. 2008; 119:326–339. [PubMed: 18662720]

11. El-Bizri N, Kahlig KM, Shyrock JC, George AL Jr, Belardinelli L, Rajamani S. Ranolazine block of human nav 1.4 sodium channels and paramyotonia congenita mutants. Channels (Austin). 2011:5.

12. Kahlig KM, Lepist I, Leung K, Rajamani S, George AL. Ranolazine selectively blocks persistent current evoked by epilepsy-associated nav 1.1 mutations. Br J Pharmacol. 2010; 161:1414–1426. [PubMed: 20735403]

13. Estacion M, Waxman SG, Dib-Hajj SD. Effects of ranolazine on wild-type and mutant hnav1.7 channels and on drg neuron excitability. Mol Pain. 2010; 6:35. [PubMed: 20529343]

14. Chambers JC, Zhao J, Terracciano CMN, Bezzina CR, Zhang W, Kaba R, Navaratnarajah M, Lotlikar A, Sehmi JS, Kooner MK, Deng G, Siedlecka U, Parasramka S, El-Hamamsy I, Wass MN, Dekker LRC, de Jong JSSG, Sternberg MJE, McKenna W, Severs NJ, de Silva R, Wilde AAM, Anand P, Yacoub M, Scott J, Elliott P, Wood JN, Kooner JS. Genetic variation in scn10a influences cardiac conduction. Nature Genetics. 2010; 42:149–152. [PubMed: 20062061]

15. Holm H, Gudbjartsson DF, Arnar DO, Thorleifsson G, Thorgeirsson G, Stefansdottir H, Gudjonsson SA, Jonasdottir A, Mathiesen EB, Njolstad I, Nyrnes A, Wilsgaard T, Hald EM, Hveem K, Stoltenberg C, Lochen ML, Kong A, Thorsteinsdottir U, Stefansson K. Several common variants modulate heart rate, pr interval and qrs duration. Nature Genetics. 2010; 42:117–122. [PubMed: 20062063]

16. Pfeufer A, van Noord C, Marciante KD, Arking DE, Larson MG, Smith AV, Tarasov KV, Muller M, Sotoodehnia N, Sinner MF, Verwoert GC, Li M, Kao WHL, Kottgen A, Coresh J, Bis JC, Psaty BM, Rice K, Rotter JI, Rivadeneira F, Hofman A, Kors JA, Stricker BHC, Uitterlinden AG, van Duijn CM, Beckmann BM, Sauter W, Gieger C, Lubitz SA, Newton-Cheh C, Wang TJ, Magnani JW, Schnabel RB, Chung MK, Barnard J, Smith JD, Van Wagoner DR, Vasan RS, Aspelund T, Eiriksdottir G, Harris TB, Launer LJ, Najjar SS, Lakatta E, Schlessinger D, Uda M, Abecasis GR, Muller-Myhsok B, Ehret GB, Boerwinkle E, Chakravarti A, Soliman EZ, Lunetta KL, Perz S, Wichmann HE, Meitinger T, Levy D, Gudnason V, Ellinor PT, Sanna S, Kaab S, Witteman JCM, Alonso A, Benjamin EJ, Heckbert SR. Genome-wide association study of pr interval. Nature Genetics. 2010; 42:153–159. [PubMed: 20062060]

17. Denny JC, Ritchie MD, Crawford DC, Schildcrout JS, Ramirez AH, Pulley JM, Basford MA, Masys DR, Haines JL, Roden DM. Identification of genomic predictors of atrioventricular conduction: Using electronic medical records as a tool for genome science. Circulation. 2010; 122:2016–2021. [PubMed: 21041692]

18. Sotoodehnia N, Isaacs A, de Bakker PI, Dorr M, Newton-Cheh C, Nolte IM, van der HP, Muller M, Eijgelsheim M, Alonso A, Hicks AA, Padmanabhan S, Hayward C, Smith AV, Polasek O, Giovannone S, Fu J, Magnani JW, Marciante KD, Pfeufer A, Gharib SA, Teumer A, Li M, Bis JC, Rivadeneira F, Aspelund T, Kottgen A, Johnson T, Rice K, Sie MP, Wang YA, Klopp N, Fuchsberger C, Wild SH, Mateo LI, Estrada K, Volker U, Wright AF, Asselbergs FW, Qu J, Chakravarti A, Sinner MF, Kors JA, Petersmann A, Harris TB, Soliman EZ, Munroe PB, Psaty

BM, Oostra BA, Cupples LA, Perz S, de Boer RA, Uitterlinden AG, Volzke H, Spector TD, Liu FY, Boerwinkle E, Dominiczak AF, Rotter JI, van HG, Levy D, Wichmann HE, Van Gilst WH, Witteman JC, Kroemer HK, Kao WH, Heckbert SR, Meitinger T, Hofman A, Campbell H, Folsom AR, van Veldhuisen DJ, Schwienbacher C, O'Donnell CJ, Volpato CB, Caulfield MJ, Connell JM, Launer L, Lu X, Franke L, Fehrmann RS, te MG, Groen HJ, Weersma RK, van den Berg LH, Wijmenga C, Ophoff RA, Navis G, Rudan I, Snieder H, Wilson JF, Pramstaller PP, Siscovick DS, Wang TJ, Gudnason V, van Duijn CM, Felix SB, Fishman GI, Jamshidi Y, Stricker BH, Samani NJ, Kaab S, Arking DE. Common variants in 22 loci are associated with qrs duration and cardiac ventricular conduction. Nat Genet. 2010; 42:1068–1076. [PubMed: 21076409]

19. Rabert DK, Koch BD, Ilnicka M, Obernolte RA, Naylor SL, Herman RC, Eglen RM, Hunter JC, Sangameswaran L. A tetrodotoxin-resistant voltage-gated sodium channel from human dorsal root ganglia, hpn3/scn10a. Pain. 1998; 78:107–114. [PubMed: 9839820]
20. Souslova VA, Fox M, Wood JN, Akopian AN. Cloning and characterization of a mouse sensory neuron tetrodotoxin-resistant voltage-gated sodium channel gene, scn10a. Genomics. 1997; 41:201–209. [PubMed: 9143495]
21. O'Brien BJ, Caldwell JH, Ehring GR, Bumsted O'Brien KM, Luo S, Levinson SR. Tetrodotoxin-resistant voltage-gated sodium channels nav1.8 and nav1.9 are expressed in the retina. The Journal of Comparative Neurology. 2008; 508:940–951. [PubMed: 18399542]
22. Jarvis MF, Honore P, Shieh CC, Chapman M, Joshi S, Zhang XF, Kort M, Carroll W, Marron B, Atkinson R, Thomas J, Liu D, Krambis M, Liu Y, McGaraughty S, Chu K, Roeloffs R, Zhong C, Mikusa JP, Hernandez G, Gauvin D, Wade C, Zhu C, Pai M, Scanio M, Shi L, Drizin I, Gregg R, Matulenko M, Hakeem A, Gross M, Johnson M, Marsh K, Wagoner PK, Sullivan JP, Faltynek CR, Krafte DS. A-803467, a potent and selective nav1.8 sodium channel blocker, attenuates neuropathic and inflammatory pain in the rat. Proceedings of the National Academy of Sciences. 2007; 104:8520–8525.
23. Antzelevitch C, Shimizu W, Yan GX, Sicouri S, Weissenburger J, Nesterenko VV, Burashnikov A, Di DJ, Saffitz J, Thomas GP. The m cell: Its contribution to the ecg and to normal and abnormal electrical function of the heart. J Cardiovasc Electrophysiol. 1999; 10:1124–1152. [PubMed: 10466495]
24. Zygmunt AC, Eddlestone GT, Thomas GP, Nesterenko VV, Antzelevitch C. Larger late sodium conductance in m cells contributes to electrical heterogeneity in canine ventricle. Am J Physiol Heart Circ Physiol. 2001; 281:H689–H697. [PubMed: 11454573]
25. Zhou X, Dong XW, Crona J, Maguire M, Priestley T. Vinpocetine is a potent blocker of rat nav1.8 tetrodotoxin-resistant sodium channels. Journal of Pharmacology and Experimental Therapeutics. 2003; 306:498–504. [PubMed: 12730276]
26. Watanabe H, Yang T, Stroud DM, Lowe JS, Harris L, Atack TC, Wang DW, Hipkens SB, Leake B, Hall L, Kupershmidt S, Chopra N, Magnuson MA, Tanabe N, Knollmann BC, George AL Jr, Roden DM. Striking in vivo phenotype of a disease-associated human scn5a mutation producing minimal changes in vitro. Circulation. 2011; 124:1001–1011. [PubMed: 21824921]
27. Liu K, Hipkens S, Yang T, Abraham R, Zhang W, Chopra N, Knollmann B, Magnuson MA, Roden DM. Recombinase-mediated cassette exchange to rapidly and efficiently generate mice with human cardiac sodium channels. Genesis. 2006; 44:556–564. [PubMed: 17083109]
28. Jarvis MF, Honore P, Shieh CC, Chapman M, Joshi S, Zhang XF, Kort M, Carroll W, Marron B, Atkinson R, Thomas J, Liu D, Krambis M, Liu Y, McGaraughty S, Chu K, Roeloffs R, Zhong C, Mikusa JP, Hernandez G, Gauvin D, Wade C, Zhu C, Pai M, Scanio M, Shi L, Drizin I, Gregg R, Matulenko M, Hakeem A, Gross M, Johnson M, Marsh K, Wagoner PK, Sullivan JP, Faltynek CR, Krafte DS. A-803467, a potent and selective nav1.8 sodium channel blocker, attenuates neuropathic and inflammatory pain in the rat. Proc Natl Acad Sci US A. 2007; 104:8520–8525.
29. Akopian AN, Souslova V, England S, Okuse K, Ogata N, Ure J, Smith A, Kerr BJ, McMahon SB, Boyce S, Hill R, Stanfa LC, Dickenson AH, Wood JN. The tetrodotoxin-resistant sodium channel sns has a specialized function in pain pathways. Nat Neurosci. 1999; 2:541–548. [PubMed: 10448219]
30. Shao D, Baker MD, Abrahamsen B, Rugiero F, Malik-Hall M, Poon WYL, Cheah KSE, Yao KM, Wood JN, Okuse K. A multi pdz-domain protein pdzd2 contributes to functional expression of

sensory neuron-specific sodium channel nav1.8. Molecular and Cellular Neuroscience. 2009; 42:219–225. [PubMed: 19607921]

31. Nuyens D, Stengl M, Dugarmaa S, Rossenbacker T, Compernolle V, Rudy Y, Smits JF, Flameng W, Clancy CE, Moons L, Vos MA, Dewerchin M, Benndorf K, Collen D, Carmeliet E, Carmeliet P. Abrupt rate accelerations or premature beats cause life-threatening arrhythmias in mice with long-qt3 syndrome. Nat Med. 2001; 7:1021–1027. [PubMed: 11533705]
32. Strauss HC, Bigger JT, Hoffman BF. Electrophysiological and beta-receptor blocking effects of mj 1999 on dog and rabbit cardiac tissue. Circulation Research. 1970; 26:661–678. [PubMed: 4393105]
33. Roden DM, Hoffman BF. Action potential prolongation and induction of abnormal automaticity by low quinidine concentrations in canine purkinje fibers. Relationship to potassium and cycle length. Circulation Research. 1985; 56:857–867. [PubMed: 4006095]
34. Manolio TA. Genomewide association studies and assessment of the risk of disease. The New England Journal of Medicine. 2010; 363:166–176. [PubMed: 20647212]
35. Yang T, Atack TC, Abraham RL, Darbar D, Roden DM. Abstract 16237: Striking electrophysiologic differences between cardiac sodium channel isoforms scn10a and scn5a. Circulation. 124:A16237.
36. Maier SK, Westenbroek RE, McCormick KA, Curtis R, Scheuer T, Catterall WA. Distinct subcellular localization of different sodium channel alpha and beta subunits in single ventricular myocytes from mouse heart. Circulation. 2004; 109:1421–1427. [PubMed: 15007009]
37. Maier SK, Westenbroek RE, Schenkman KA, Feigl EO, Scheuer T, Catterall WA. An unexpected role for brain-type sodium channels in coupling of cell surface depolarization to contraction in the heart. Proceedings of the National Academy of Sciences. 2002; 99:4073–4078.
38. Facer P, Punjabi PP, Abrari A, Kaba RA, Severs NJ, Chambers J, Kooner JS, Anand P. Localisation of scn10a gene product na(v)1.8 and novel pain-related ion channels in human heart. Int Heart J. 2011; 52:146–152. [PubMed: 21646736]
39. The CI. Preliminary report: Effect of encainide and flecainide on mortality in a randomized trial of arrhythmia suppression after myocardial infarction. New England Journal of Medicine. 1989; 321:406–412. [PubMed: 2473403]
40. Morrow DA, Scirica BM, Karwatowska-Prokopczuk E, Murphy SA, Budaj A, Varshavsky S, Wolff AA, Skene A, McCabe CH, Braunwald E. Investigators FtM-TT. Effects of ranolazine on recurrent cardiovascular events in patients with non–st-elevation acute coronary syndromes. JAMA: The Journal of the American Medical Association. 2007; 297:1775–1783. [PubMed: 17456819]
41. Scirica BM, Morrow DA, Hod H, Murphy SA, Belardinelli L, Hedgepeth CM, Molhoek P, Verheugt FWA, Gersh BJ, McCabe CH, Braunwald E. Effect of ranolazine, an antianginal agent with novel electrophysiological properties, on the incidence of arrhythmias in patients with non st-segment elevation acute coronary syndrome: Results from the metabolic efficiency with ranolazine for less ischemia in non st-elevation acute coronary syndrome thrombolysis in myocardial infarction 36 (merlin-timi 36) randomized controlled trial. Circulation. 2007; 116:164–1652.
42. Wu L, Shryock JC, Song Y, Li Y, Antzelevitch C, Belardinelli L. Antiarrhythmic effects of ranolazine in a guinea pig in vitro model of long-qt syndrome. Journal of Pharmacology and Experimental Therapeutics. 2004
43. Antoons G, Oros A, Beekman JD, Engelen MA, Houtman MJ, Belardinelli L, Stengl M, Vos MA. Late na(+) current inhibition by ranolazine reduces torsades de pointes in the chronic atrioventricular block dog model. J Am Coll Cardiol. 2010; 55:80–809.
44. Burashnikov A, Belardinelli L, Antzelevitch C. Atrial-selective sodium channel block strategy to suppress atrial fibrillation: Ranolazine versus propafenone. The Journal of pharmacology and experimental therapeutics. 2012; 340:16–168.

Novelty and Significance

What is Known?

- Genome-wide association studies have implicated variation in the sodium channel gene *SCN10A* as modulators of cardiac conduction (PR and QRS durations)
- *SCN10A* was originally cloned from dorsal root ganglion, and the encoded channel (termed Nav1.8) is thought to play a role in pain perception

What New Information Does This Article Contribute?

- A specific Nav1.8 blocker eliminates the persistent sodium current recorded after long depolarizing pulses in mouse and rabbit cardiomyocytes and shortens the action potential duration.
- These effects are absent in myocytes from *Scn10a* knockout mice.
- The Nav1.8 blocker reverses arrhythmogenic early afterdepolarizations elicited by experimental conditions that increase persistent sodium current.

Genome-wide association studies of cardiac conduction suggest a role for variation in *SCN10A*, not previously implicated in heart function. We show that *Scn10a* transcripts are present in the mouse heart. Also, we confirmed the selectivity of the Nav1.8 blocker A-803467 over Nav1.5 encoded by the canonical cardiac sodium channel gene *SCN5A*. In mouse and rabbit ventricular myocytes, a low concentration of A-803467 had little effect on peak sodium current but eliminated “late” current recorded after a long depolarizing pulse, and shortened action potential duration. These effects were absent in cells from *Scn10a0* knockout mice. The blocker also eliminated arrhythmogenic early afterdepolarizations elicited when the late current was increased. These results identify a role for the *SCN10A*gesssne product in mediating late current in the heart, and suggest that inhibition of this current may be antiarrhythmic under some conditions.

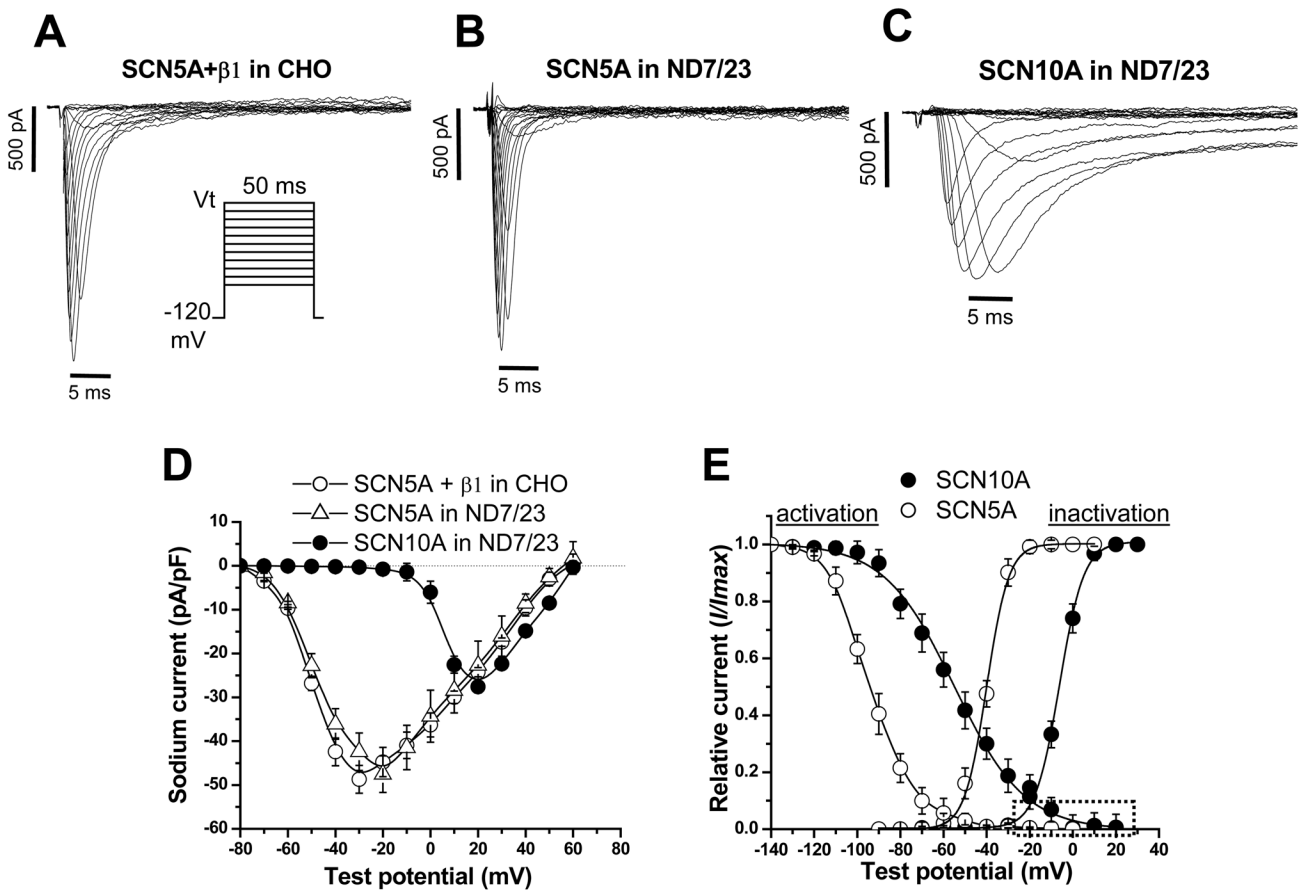

Figure 1. Comparison of human cardiac Nav1.8 and Nav1.5 currents in heterologous expression systems

A, Nav1.5 recorded in *SCN5A*+*SCN1B* (β1) co-transfected CHO cells. The voltage clamp protocol is shown in the inset. **B,** Nav1.5 recorded in *SCN5A*-transfected ND7/23 cells. The similarity between currents in this panel and panel a support previous reports that ND7/23 cells express endogenous β1 and β3 subunits. **C,** Nav1.8 recorded in *SCN10A*-transfected ND7/23 cells. Nav1.8 activates and inactivates much more slowly than does Nav1.5. **D,** Current-voltage curves showing that *SCN10A* current activates at much more positive potentials than does SCN5A current. **E,** Voltage dependence of activation and inactivation of Nav1.8 and Nav1.5 in ND7/23 cells. In *SCN10A* channels, the area of overlap (dotted box) under the activation and inactivation curves is much larger than that for *SCN5A*, suggesting that *SCN10A* channels generate an increased 'window" current. N=6 for *SCN5A* and N=9 for *SCN10A*.

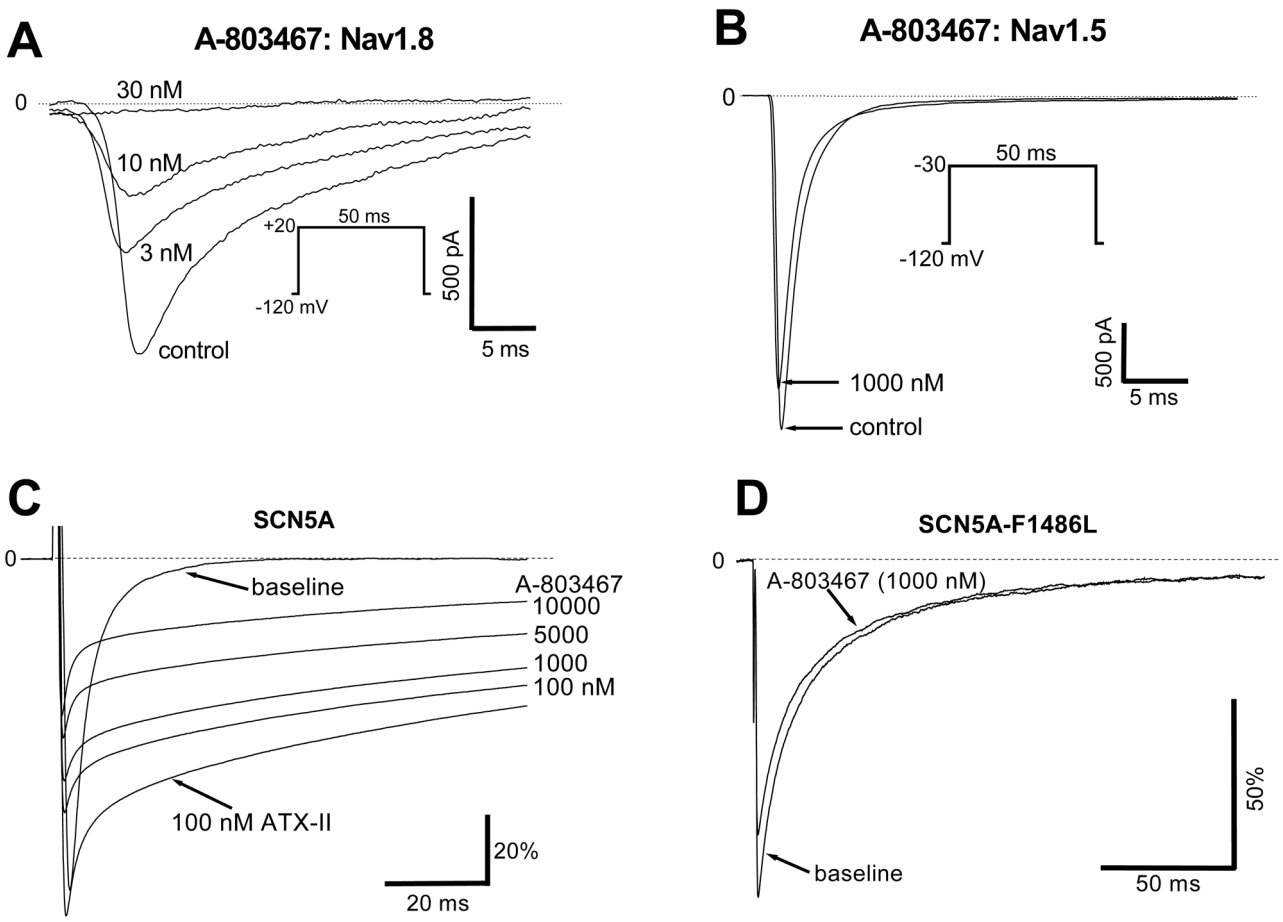

Figure 2. A-803467 is a potent Nav1.8 blocker with minimal effect on Nav1.5

A, Near total inhibition of Nav1.8 current by low concentrations of A-803467 in an *SCN10A*-transfected ND7/23 cell. **B,** Minimal effect of A-803467 on Nav1.5 current in an *SCN5A*-tranfected ND7/23 cell. **C,** Late current was first elicited by 100nM ATX-II in an *SCN5A*-transfected ND7/23 cell, and then the effect of increasing concentrations of A-803467 were examined; the IC_{50} was ~5000 nM. Under the same conditions, the IC_{50} for block of late *SCN10A* currents was ~10 nM **D,** The LQT3 mutant F1486L generated a large late I_{Na} in CHO cells, and this was unaffected by 1000 nM A-803467. The same lack of effect was seen with late I_{Na} generated by R1544H and T1304M (data not shown).

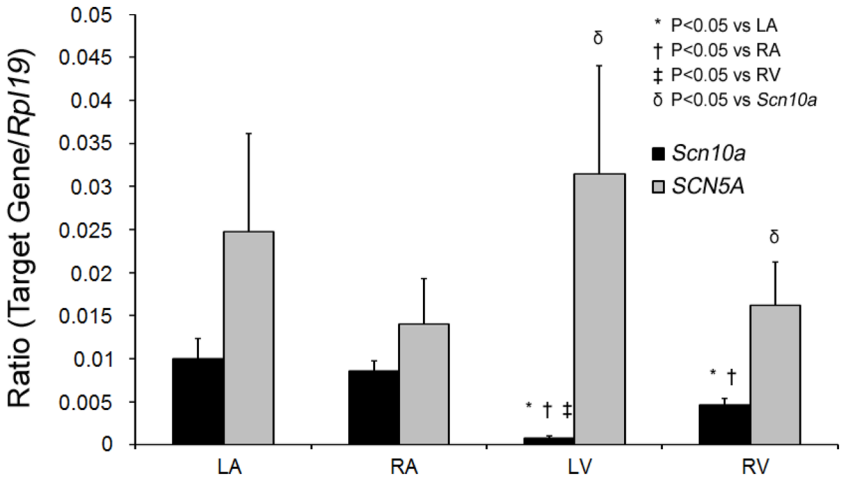

Figure 3. Quantitative PCR showing relative expression of *Scn10a* to *SCN5A*

Data for both genes were normalized to those for the housekeeping gene *Rpl19. Scn10a* expression was significantly lower than in the atria and was markedly lower in left versus right ventricle. N=4 hearts. LA, Left atria; RA, right atria; LV, left ventricle; RV, right ventricle.

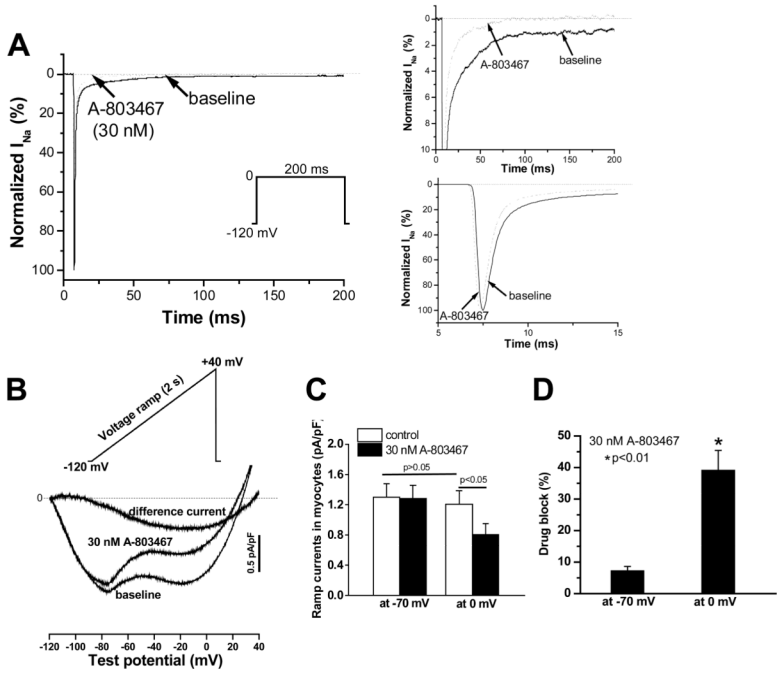

Figure 4. Effect of A-803467 on sodium current (I_{Na}) in mouse ventricular myocytes

A, Sodium current traces elicited by repetitive 200-ms square pulses from −120 mV to 0 mV in a ventricular myocyte in the absence (solid traces) and presence (dotted traces) of the blocker; current is normalized as I/I_{max} (%), where I_{max} is peak inward current pre-drug. The panels on the right highlight at expanded scales the effect of the drug to selectively and near-completely inhibit late current but to exert minimal effect on peak sodium current, consistent with the idea that peak current represents predominantly *SCN5A* current. **B,** Using a ramp protocol reveals that the drug prominently blocked late current at more positive potentials. The A-803467 sensitive current was obtained by digital subtraction. **C,** Summary data for ramp experiments show the effects of the drug on the ramp currents at −70 and 0 mV (n=8). **D,** Preferential suppression of the late current at 0 mV by the drug.

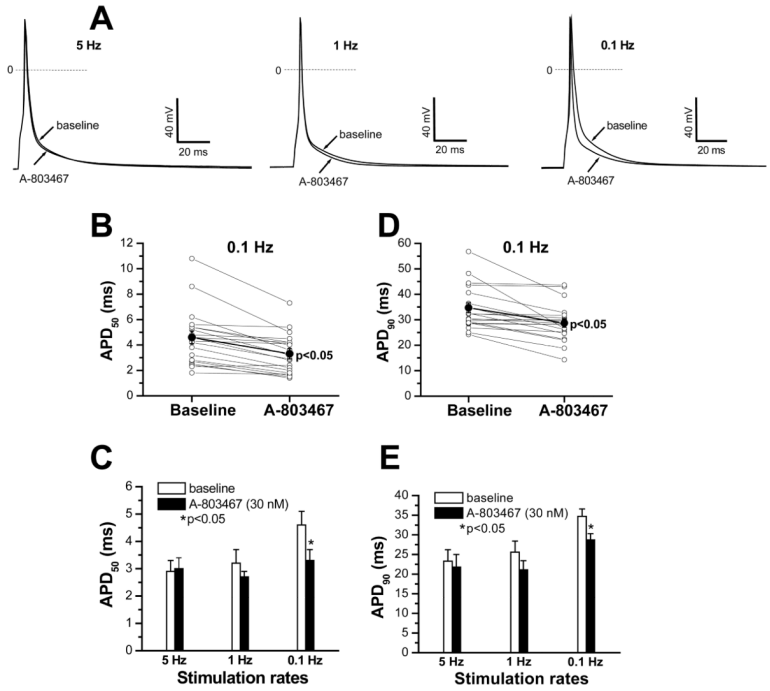

Figure 5. Effects of A-803467 on action potentials in mouse ventricular myocytes

A, Representative action potential traces showing the effects of 30 nM A-803467 at 5, 1 and 0.1 Hz. **B,** Individual action potential duration (APD) values measured at 50% repolarization (APD_{50}) in 20 ventricular myocytes stimulated at 0.1 Hz are shown pre- and post-drug ($p<0.05$). **C,** Summary data for APD_{50} values obtained at the different stimulation rates. **D,** Individual APD values measured at 90% repolarization (APD_{90}) in 20 ventricular myocytes stimulated at 0.1 Hz are shown pre- and post-drug ($p<0.05$). **E,** Summary data for APD_{90} values obtained at the different stimulation rates (n=20).

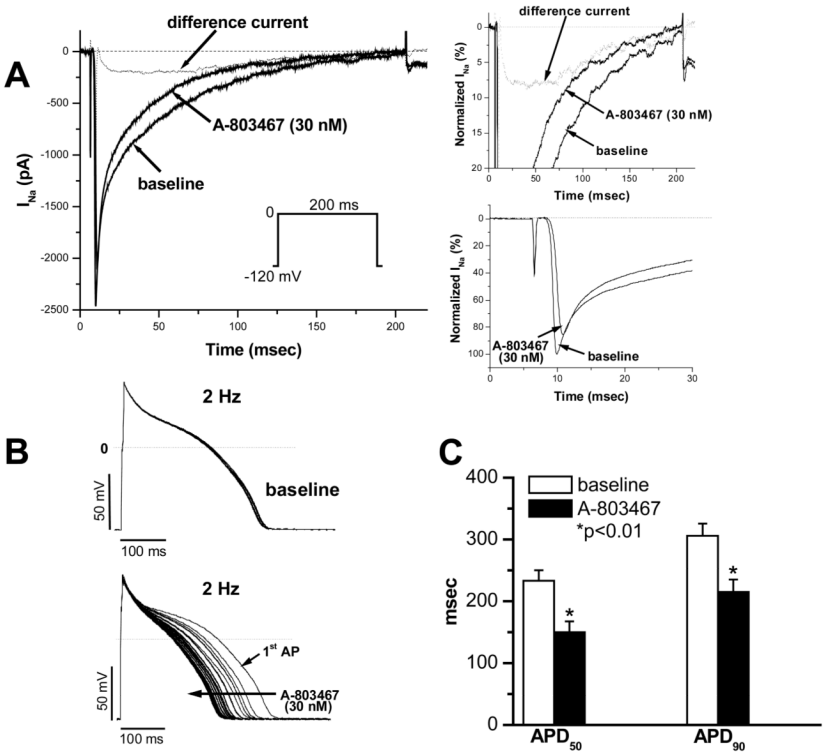

Figure 6. Effects of A-803467 on late current and action potential duration in rabbit ventricular myocytes

A, Sodium current traces elicited by repetitive 200-ms square pulses from −120 mV to 0 mV in a ventricular myocyte in the absence and presence of the blocker; the current component blocked by A-803467 is indicated by difference current obtained by digitally subtracting the currents pre- and post-drug. The panels on the right highlight at expanded scale the effect of the drug to selectively inhibit late current with a slowly-activating and slowly-inactivating difference current and minimal effect on peak sodium current, consistent with the idea that peak current represents predominantly Nav1.5 current. The insets are presented as percentages after normalization to peak sodium current. **B,** Action potential traces recorded with repetitive stimulation at 2 Hz prior to drug (top) and during exposure to 30 nM A-803467 (bottom). **C,** Summary of action potential durations (APD_{50} and APD_{90}) in the absence and presence of A-803467.

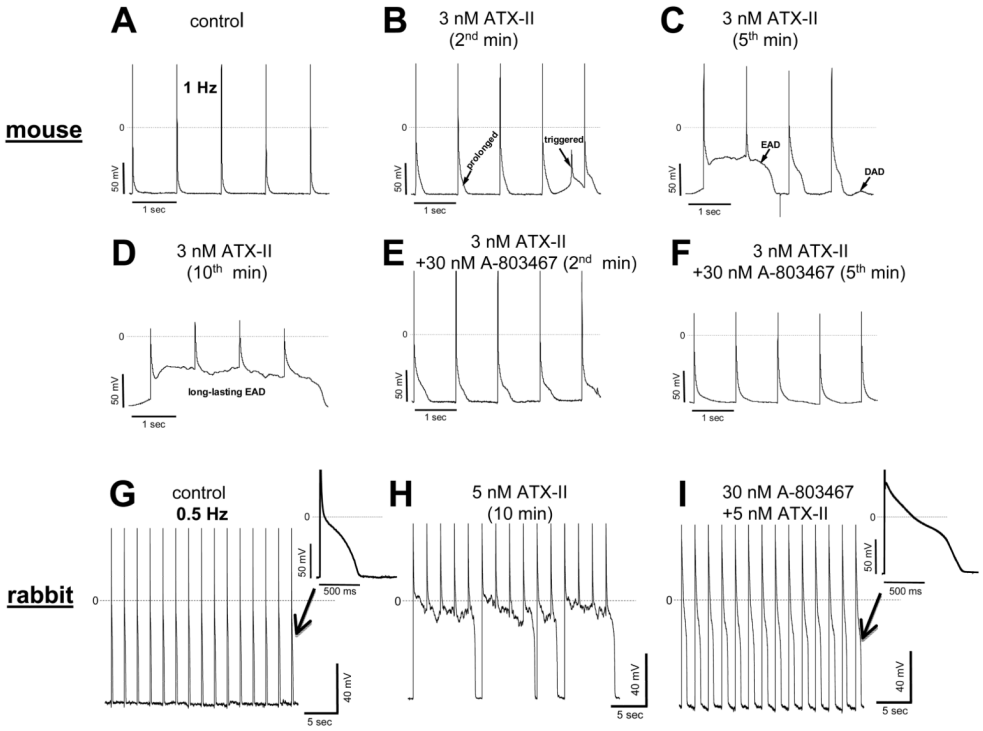

Figure 7. Antiarrhythmic effects of A-803467 in mouse and rabbit ventricular myocytes

A–F, Changes in action potentials recorded at 1 Hz in the absence and presence of ATX-II alone and then ATX-II + A-803467 in a mouse myocyte. **G** and **H,** ATX-II induced long-lasting early afterdepolarizations (EADs) at 0.5 Hz in a rabbit myocyte. **I,** pretreatment of a rabbit myocyte with A-803467 eliminated ATX-II induced EADs. Two action potential traces indicated by arrows are for comparison.

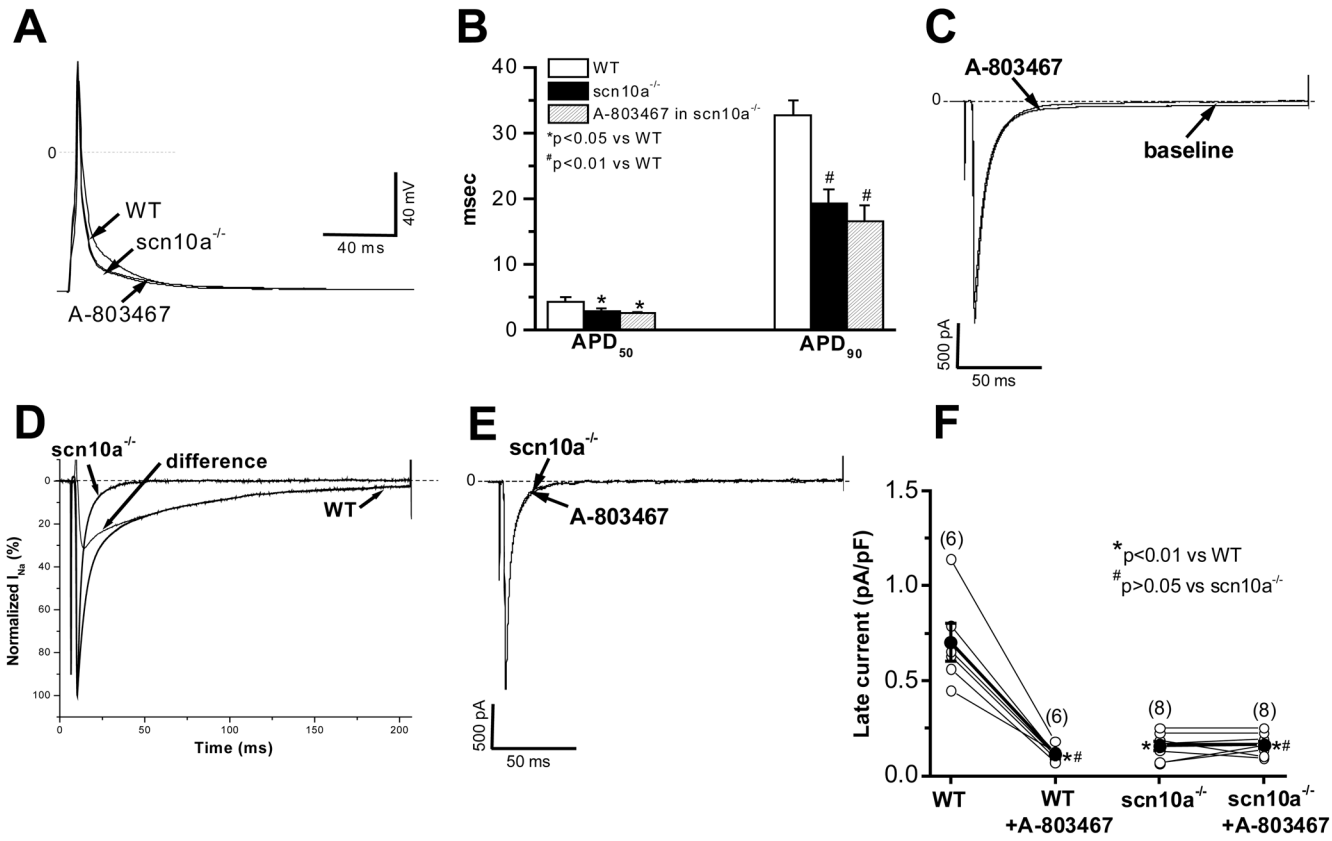

Figure 8. Action potential durations and late current in scn10a$^{-/-}$ mouse ventricular myocytes

A, Action potential recordings at a simulation rate of 0.1 Hz in a WT (H/H) cell and in an *Scn10a*$^{-/-}$ cell prior to and during exposure to 30 nM A-803467. **B**, Summary of action potential durations (APD_{50} and APD_{90}) in myocytes (n=8 each) under conditions as shown in panel A. **C**, In same WT myocyte, 30 nM A-803467 abolished late current at 0 mV, with a minor reduction of peak current. **D**, Normalized sodium current traces recorded at 0 mV from two separate myocytes from WT and *Scn10a*$^{-/-}$ mice. Difference current is a component obtained by digital subtraction of these two traces. This difference current resembles the Nav1.8 current seen in Figure 1C and A-803467 sensitive current in Figure 6A. **E**, In same *Scn10a*$^{-/-}$ myocyte, adding 30 nM A-803467 had no effect on sodium current. **F**, Individual and summarized late current data after normalization to cell size (in pA/pF) in individual myocytes studied prior to and during exposure to 30 nM A-803467. Solid circles represent the mean value (±SEM) for each groups.